*Bangladesh Journal of Physics, Vol. **27**, Issue 1, pp. 1–12, 2020*

Invited Paper

FE DOPED MnO_2 NANOSTRUCTURED THIN FILMS: SYNTHESIS AND CHARACTERIZATION FOR BIOSENSOR APPLICATIONS

M. ZAHAN AND J. PODDER*

Department of Physics, Bangladesh University of Engineering and Technology, Dhaka-1000, Bangladesh

**Corresponding author e-mail: jpodder@phy.buet.ac.bd*

Received on 24.07.2020, Accepted for publication on 28.07.2020

DOI: https://doi.org/10.3329/bjphy.v27i1.49722

ABSTRACT

Iron (Fe), a magnetic transition metal, doped manganese oxide (MnO_2) nanostructured thin films were deposited onto glass substrates by a spray pyrolysis deposition technique at 450 °C substrate temperature for glucose sensing performance. Fe concentration greatly affects the film surface morphology. The film was found to be more compact and porous for 4 at % Fe doping. The glucose response was measured by electrical four probe method using the pure MnO_2 and 2, 4, 6, 8 at% Fe doped MnO_2 thin films as an active electrode. It was determined that 4 at % Fe: MnO_2 thin film with 20 nm crystallite size has high sensitivity, fast glucose response and recovery time. Optical band gap measurement indicated that the sensitivity increased as the band gap decreased up to 4 at% Fe concentration. The highest glucose sensing response was recorded about 29 % in 5 minutes.

Keywords: MnO_2; Spray pyrolysis; Nanostructured thin film; FESEM; Glucose sensing.

1.1 INTRODUCTION

Manganese oxide (MnO_2) is a common transition metal oxide with multiple valences, high capacitance, natural abundance, environmental friendliness and p-type charge carrier. Nanostructured thin films of Fe doped MnO_2 show various properties of crystal structure, crystallite size, suitable optical band gap, moderate magnetizations, high coercivities, single domain effects, etc. [1]. Such nanostructured thin films have many applications in the field of photocatalysis, gas sensors, water treatment, protective coating on optical elements and biological sciences [2]. Among sensor groups, biosensor has a very important role in the field of medicine, biology and biotechnology. The development of glucose sensor has received continuous interest. Semiconductor metal-oxide-based glucose sensors are used for environmental, automotive, domestic, industrial and medical applications. The glucose sensing mechanism in these materials is governed by the reactions which occur at the sensor surface (active layer) and glucose molecules. It involves chemisorption of oxygen on the oxide surface followed by charge transfer during the reactions of oxygen with glucose molecules. The adsorbed glucose atoms extract electrons or inject electrons into the semiconducting material, depending on whether they are reducing or oxidizing agents, respectively [3-4]. This mechanism results in a change of the film conductivity, which corresponds to the glucose concentration. The performance of a glucose sensor is directly related to porosity, and ratio of exposed surface area to volume. Recent advances in the synthesis, structural characterization, and

investigation of physical properties of nanostructured metal oxides provide the opportunity to greatly improve the response of these materials for glucose sensing. Among the semiconductor metal oxides, MnO_2 is the most widely applied oxide sensing materials due to its high mobility of conduction electrons and good chemical and thermal stability under operating conditions [5]. Various growth techniques have been reported in literature, such as wet chemical process [6], atomic layer deposition [7], pulsed laser deposition [8], metal-organic vapor phase epitaxy [9], electrochemical deposition [10], dip coating [11], spray pyrolysis technique (SPT) [12] and sputtering [13] for fabricating nanostructured MnO_2 thin film. The main objective of this work is to find out the surface morphological, structural, optical and electronic properties of MnO_2 thin films synthesized via spray pyrolysis method and to see the effect of Fe doping concentrations on the nanostructured MnO_2 thin films for fast and precise detection of glucose response in concentration.

2. SYNTHESIS AND PROCESSING

2.1 Synthesis

The analytical grade manganese (II) acetate tetra-hydrate [$Mn(CH_3COO)_2.4H_2O$](Merck, Germany, 99.5% purity) and $FeCl_3$were used as the starting materials. Deionized distilled water was used as a solvent and hydrochloric acid (HCl) as a stable reagent. D-glucose ($C_6H_{12}O_6$) and sodium hydroxide (NaOH) were used as precursors for sensitivity measurements. In this study Fe doped MnO_2 thin films with various Fe concentrations of 0, 2, 4, 6 and 8 at% were synthesized on plain glass substrate of area 5 × 2.5 cm^2 with a suitable mask by an SPT. The substrates were soaked with acetone and distilled water in an ultrasonic cleaner for 30 min and subsequently dried in flowing hot air to execute a better adherence between the film and the substrate.

2.2 Processing

In a typical procedure, for pure MnO_2, 0.1 M of $Mn(CH_3COO)_2{\cdot}4H_2O$ was prepared in 100 mL of double distilled water including few drops of C_2H_5OH and the mixed solvent was stirred about 1 h to form a homogeneous fuscous slurry. For Fe doped MnO_2 (Fe:MnO_2), 0.1 M of $Mn(CH_3COO)_2{\cdot}4H_2O$ and $FeCl_3$ powder were mixed into 100 mL of double distilled water including few drops of hydrochloric acid (HCl) as a stable reagent. After that, the solution was filtered and then sprayed through a fine bore in the form of fine droplets on pre-heated commercial glass substrates with a deposition time of 20 min. The temperature of the substrate was kept at 450 °C constant. The distance between the spray nozzle and the substrate was kept at 25 cm. The pressure of air as the carrier gas was maintained at 0.5 bar. The spray rate was maintained at 0.5 mL min^{-1} throughout the experiment. After deposition, the thin films were allowed to cool to room temperature. The as-deposited MnO_2 and Fe: MnO_2 thin films were found homogeneous and brown in color.

2.3 Characterization

Field Emission Scanning Electron Microscope (FESEM) images were taken using JEOL JSM-7600F, operated at 20 kV under x100000 magnification and 100 nm scale bar lengths. The XRD spectra of the deposited films was recorded using a powder X-ray Diffractometer (model: PANalytical Empyrean series 2, using CuK_α radiation (λ = 1.54056Å) with a diffraction angle between 10° to 90°. The crystallite size was determined from the broadenings of corresponding X-ray peaks by using Debye-Scherer's formula. Glucose sensitivity was determined by four probe method.

3. RESULTS AND DISCUSSION

3.1 Structural characterization

The surface morphology of pure MnO_2 and 4 at% Fe: MnO_2 is shown in Figure 1a and 1b, respectively. Figure 1a shows agglomerated nanoparticles and 1b porous surface. It is seen from the images that the surface quality of the films is good and have no cracks. It is seen in Figure 1a that the thin films consist of grains and the grains are of close-packed structure with round shape. Granular agglomerated nanoparticles are trotted out from the porous surface of 4 at% Fe: MnO_2 thin films as displayed in Figure 1b [14].

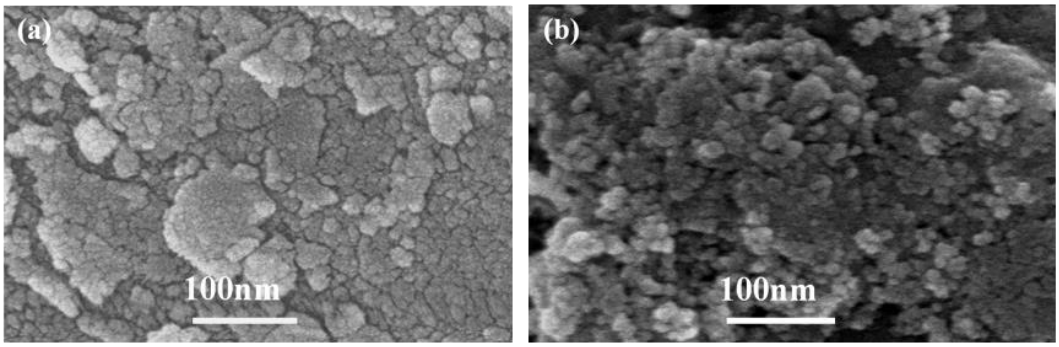

Fig. 1. (a) Pure MnO_2 agglomerated nanoparticles, and (b) 4 at% Fe: MnO_2, porous surface.

The unit cell of the crystal system was found to be the tetragonal structure with dominant peaks at (310), (101), (211) planes without any secondary phase as displayed in Figure 2. When Fe is introduced, the intensity of the three prominent peaks is changed. The variation in intensity indicates the incorporation of Fe ions into the lattice site of MnO_2. In the doping process, the three prominent peaks are shifted from higher to lower angles due to the different ionic radii of $Fe^{3+}$and Fe^{2+} . For 4% Fe, the (002) peak shifts to lower angle due to the high ionic radius of Fe^{2+} (70 pm). FESEM analysis also revealed that Fe concentration strongly influenced the grain size of the thin films. The crystallite size was estimated in the range of 20 nm to 30 nm using the Debye Scherer relation. The density of defects in the sample, termed as dislocation density (δ) which stands for the length of dislocation lines per unit volume of the crystal, has been calculated by $\delta = \frac{1}{D^2}$ [15]. The XRD data suggest that Fe: MnO_2 has a lower crystallization due to the disorders or defects of lattices resulting from the excessive Fe dopants. The reason is that iron oxide is an amorphous nature and can influence the crystalline nature of α-MnO_2. The effect of Fe concentration on the dislocation density, crystallite size, and strain (ε) in the MnO_2 crystal lattice along (101) is presented in Table 1.

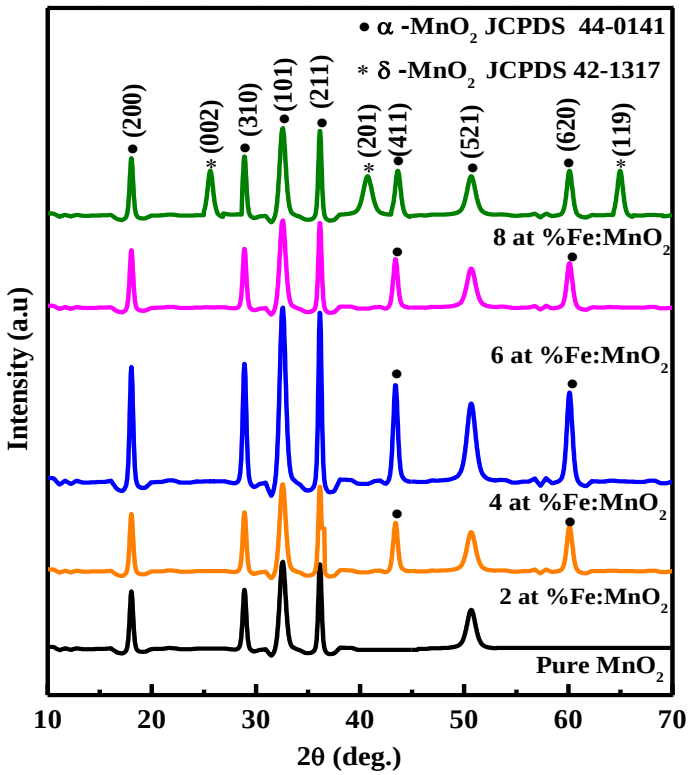

Fig. 2. X-ray diffraction patterns of pure MnO_2 and 2, 4, 6 and 8 at % Fe doped MnO_2 thin films.

Table 1. Variation of structural parameters with Fe doping concentration

Fe at%	D (nm)	a=b (Å)	c (Å)	Strain $\varepsilon \times 10^{-3}$	$\delta \times 10^{-3}$ (lines/nm^2)
0	24	9.852	2.863	1.423	1.736
2	22	9.822	2.861	1.512	2.066
4	20	9.798	2.862	1.835	2.500
6	28	9.778	2.860	1.137	1.276
8	30	9.762	2.859	0.996	1.111

With 2 at% Fe-doped MnO_2 thin films, the intensity of the peaks is reduced and FWHM is increased in comparison to undoped MnO_2 thin films revealing that the crystalline quality is weakened by introducing dopant. On the other hand, when the Fe-doping concentration is above 4 at%, (viz. 6 and 8 at%), crystalline quality is weakened again, indicated by the reduction of peak intensity and increased FWHM value in comparison to lower doping concentrations. This happens due to the creation of new nucleation centers from the dopant atoms is favorable for the growth of MnO_2 crystals. However, the crystalline quality is degraded further when the Fe-doping concentration is 8 at%. This may occur as the newer nucleation centers reach in saturation and due to the difference of

ionic radius between Fe^{+2} or Fe^{+3} and Mn^{+2} and large number of Fe^{+2} or Fe^{+3} replace Mn^{+2} in lattice sites. The ionic radii of Fe^{+2}, $Fe^{+3}$and Mn^{+2} are 70, 60 and 70 pm, respectively. Fe^{+2} or Fe^{+3} replacing Mn^{+2} in lattice sites will lead to lattice distortion which results in a strain in MnO_2 thin films. When Fe ions exist in MnO_2 mostly in the form of Fe^{+2}, due to its larger ionic radius than that of Mn^{+2}, will lead to compression strain in the films. Therefore, XRD patterns shift towards the smaller angle. On the contrary, if Fe ions exist in MnO_2 mainly in the form of Fe^{+3} due to its smaller ionic radius than that of Mn^{+2}, will lead to tensile strain in the films, producing a shifting of the peak towards higher angle. In Fe: MnO_2 alloys, Fe ions require having a valence of +2 in order to properly substitute Mn^{+2} ionic sites while maintaining charges neutrality. When Fe^{+3} ions coexist with Fe^{+2} ions in Fe: MnO_2, the Fe^{+3} ions are likely to distort the lattice structure for holding charge neutrality

3.2 Optical properties

The optical band gap of MnO_2 and Fe: MnO_2 films were calculated using Tauc relation. The optical band gaps of Fe: MnO_2 films are shown in Figure 3. The optical energy gap was obtained by extrapolating the linear part to *x*-axis. The energy gap reduces due to the increase in Fe doping concentration indicating the red shift [16]. Band gap decreases gradually up to 4 at% Fe doping due to s-p and p-d exchange interaction between Mn^{+2} and Fe^{+2} ions. At 6 at% Fe doping, band gap starts to increase due to phase transformation from α to δ [12]. Reduction of band gap may also be from p-d exchange interaction between Mn^{+2} and Fe^{+2} ions.

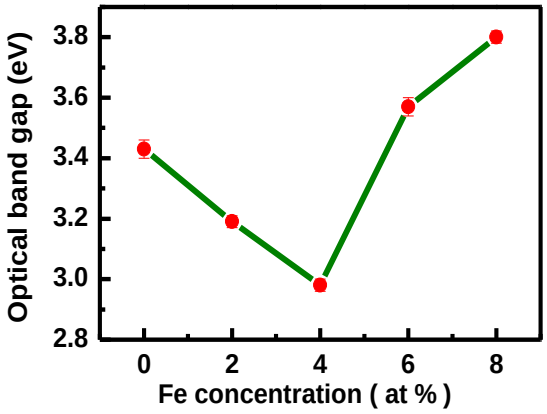

Fig. 3. Band gap versus different Fe %.

Table 2 Band gap versus different Fe %

Fe concentration (at %)	Band gap (eV)
0	3.31
2	3.19
4	2.98
6	3.29
8	3.43

3.3. Electrical characterization

The variation of electrical resistivity (ρ) with temperature ranging from 27-150 ºC for pure and 2, 4, 6 and 8 at % Fe doped MnO_2 thin films revealed that resistivity decreased with the increase of temperature. This type of variation indicates the semiconducting behavior of the films. In a polycrystalline oxide semiconductor, oxygen adsorption and desorption may occur at all temperatures when heat treated in air. The decrease in electrical resistivity may be due to oxygen decomposition process into the deposited film. Table 3 shows the data of resistivity (P), carrier concentration (n), and mobility (μ), and Hall coefficient (R_H).

Table 3. Hall parameters of Fe:MnO_2 thin films variation with Fe concentrations

Fe at%	ρ ($\times 10^3 \Omega$-m)	n ($\times 10^{17}$ cm^{-3})	μ ($cm^2 V^{-1} s^{-1}$)	R_H (cm^3C^{-1})
0	3.56	3.29	2.81	1.97
2	2.17	3.86	2.32	1.53
4	1.95	4.13	1.87	1.32
6	3.88	4.02	1.99	1.68
8	4.79	3.71	2.17	1.83

The carrier concentration raise and Hall mobility drops from pure to 4 at % Fe doping. It is evident that the relatively low resistivity at of pure MnO_2, compared to that of 4 at % Fe doping is mainly due to the increase of carrier concentration with some contribution from the decrease of mobility. This variation may for the sake of amount of oxygen vacancies. So if the oxygen vacancy was the dominant factor, its drop should have resulted in an increase in mobility, contrary to the Hall measurement.

3.4 Sensing properties

MnO_2 thin films can be used for the sensing of the several biomolecules such as antibody, enzyme, receptor protein, nucleic acid, glucose, whole cell or tissue section etc. The sensing mechanism of glucose based on the Fe: MnO_2 thin films are primarily related with variation of active layer conductivity under glucose molecules [17]. Changing of their electrical properties interested in adsorption of oxygen by trapping an electron from the conduction band of the MnO_2 semiconductor. Glucose sensing depends on the air oxidation of glucose molecules on the surface of the film layer and decomposition into glucono lactone ($C_6H_{10}O_6$) and hydrogen peroxide (H_2O_2). Oxidation of glucose molecules on the surface of the film results in hydrogen peroxide molecules which pass through the porous thin film and adsorb on the surface of the counter electrode layer. In this study the sensing ability of the prepared thin films with respect to glucose ($C_6H_{12}O_6$) was evaluated by four probe method where Fe: MnO_2 thin film was the working electrode. In the glucose ($C_6H_{12}O_6$) solution, NaOH is added to accelerate the current to reach a stable state as glucose and OH^- aqueous ions are adsorbed in the film surface as,

$$C^6H^{12}O^6 + H^2O + NaOH \rightarrow C^6H^{10}O^6 + O^2 + H_+ + 2e^-$$

In our experiment we measured the current through the as-deposited thin films with and without glucose solutions to check the response of the film. At first, the current through the Fe doped MnO_2 thin films was measured (without glucose solution) applying constant supply voltage (+64V) varying with time. Then glucose solution was set with the working electrode and current was

measured under the same conditions and observed the variation in current values. With the variation in current values, the glucose sensing abilities of the deposited thin films were confirmed and sensitivity was calculated using the formula:

$$S\ (\%) = \left|\frac{I_g - I_a}{I_g}\right| \times 100$$

Where $I_a$the current of the sensor in air and I_g is the current under diffusive glucose. The dynamic properties of the sensor such as sensitivity, stability, response, and recovery times were all found to be time, Fe concentration and glucose concentration dependent.

3.4.1 Sensing measurements

In this experiment, recovery and response times on the variation of the sensing current of pure MnO_2 and 4 at% Fe: MnO_2 were observed with and without introduction of glucose. At first, for pure MnO_2 and 4at% Fe: MnO_2, sensors' current was recorded in 5 minutes in air. Then, the current was observed with 0.2 M $C_6H_{12}O_6$ glucose and found that current was sharply increased and after that, rapidly recovered the initial value. This result indicated that fabricated MnO_2 sensor has a good response time. For determining the reproducibility, this process was repeated. Figures 4a and 4b show the typical current-time response plot of pure and 4 at % Fe: MnO_2 thin films, respectively.

It was observed that with the increase of time, the response and recovery times of the sensor were increased. It is clearly observed that the sensing current is increased with the Fe concentration and maximum current response is obtained at 4 at% Fe doping. This may be due to the incorporation of Fe into MnO_2 and having more active sites for the detecting of glucose, displaying a shorter time. Both MnO_2 and Fe: MnO_2 act as active electrodes showing high current response with glucose solution and no noise was found as displayed in Figures 4a and 4b.

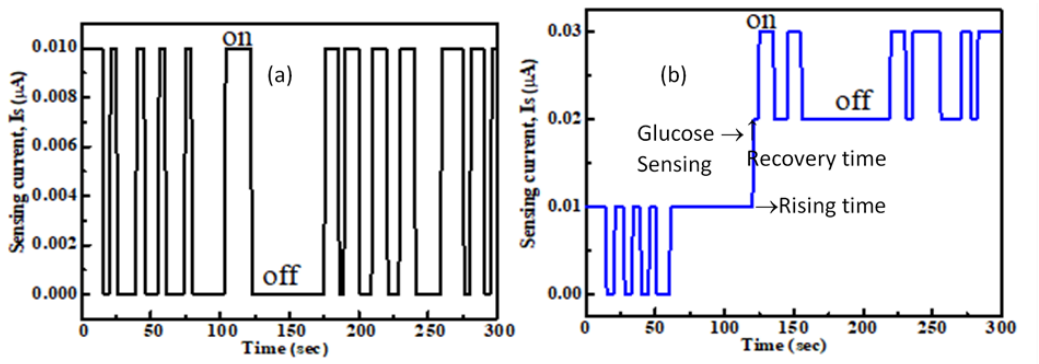

Fig. 4. Current-time response plot of (a) pure MnO^2,(b) 4 at% Fe: MnO^2.

The reason of the phenomenon for the observed waveform is that the current of the prepared thin films changed when the aqueous glucose was adsorbed. This waveform shows a significant response which is clearly demonstrated by the change in current of undoped and Fe doped MnO_2 thin films. MnO_2 become more sensitive with a fast response in the presence of Fe which may due to their

unique surface properties such as a high surface area and a high pore density of surface that facilitate the transport of reactant (glucose) molecules and to enhance sensing performance. The main influence of glucose sensing properties to improve in the case of doped materials is also for enhancing the electrical properties. This leads to an increase of the electron concentration which eventually increases the oxygen vacancies-related defects in MnO_2 nanoparticles. Therefore, more adsorption sites for glucose (liquid) molecules are provided by these oxygen vacancies causing the surface to be highly active for reaction so that sensing properties are improved. The rectangular response shown in Figure 4 confirms that there is no negative influence of D-glucose ($C_6H_{12}O_6$) on the sensing performance of Fe dopedMnO_2 thin films. Furthermore, high supply voltage and low glucose concentration may responsible for rectangular response. The sudden increase and decrease in current may occur by means of complete oxidation-reduction of glucose through film surface due to the effect of high supply voltage. A slight increase in current can be explained by a partial oxidation of glucose. In this system the film acts as an electron transmitter where electron conversion is occurred at high potential on the surface of the film. On the other hand at lower glucose concentration (≤ 1mol/ L) there is absence of any noise and the stages are well-formed which indicates a complete glucose oxidation. Hence glucose is deprotonated to gluconolactone ($C_6H_{10}O_6$) in alkaline (NaOH) assisted aqua solution and adsorbs to the catalytic active film surface.

3.4.2 Measurements of response time

The response time was measured from the plot of time vs sensing current (with glucose) as shown in Figure 5. Figures 5 (a) and (b) show the response time of pure MnO_2 and 4 at% Fe doped MnO_2 thin films electrode as 1.13 s and 1.02 s, respectively. Which may be due to the incorporation of Fe into MnO_2, the Fe: MnO_2 may own more active sites for the detecting of glucose, displaying a shorter time for the detecting of glucose.

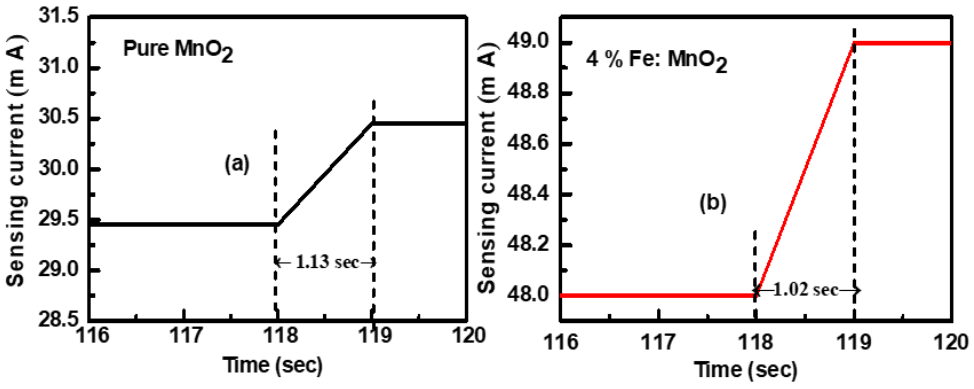

Fig. 5. Response time of (a) pure MnO_2 and (b) 4at% Fe: MnO^2.

3.4.3 Sensitivity with Fe concentration

Figure 6 (a) shows the glucose response of pure MnO_2 and 4 at% Fe doped MnO_2 thin films. The response was dramatically increased with the increase of Fe concentration especially for 4 at% than other concentrations. The sensitivity of the thin films prepared in this study is found higher than those in previous reports of spin-coated or electrodeposited MnO_2 films [18].

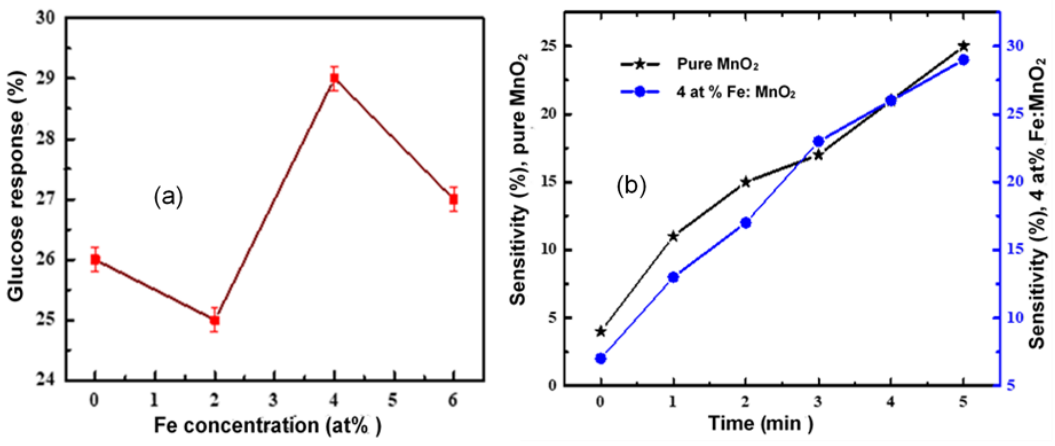

Fig. 6. (a) Glucose sensitivity variation with Fe concentration at 5 minutes, and (b) Glucose sensitivity of pure MnO_2 and 4 at% Fe:MnO_2 variation with time.

3.4.4 Sensitivity with time

The Fe: MnO_2 electrode exhibited better sensitivity for glucose detection than pure MnO_2 film shown in Figure 6(b). Higher sensitivity may occur by means of higher surface area to volume ratio of the Fe:MnO_2 than surface area of MnO_2 for catalytic activity. However, the Fe:MnO_2 electrode showed a higher detection than that of MnO_2 because Fe: MnO_2 showed more rising and recovery times than that of MnO_2. Fe ions may be distributed homogeneously throughout the porous surface of Fe:MnO_2 electrode. As a result local electron transfers due to redox reaction through the Fe:MnO_2 surface resulting higher detection of 4 at % Fe concentration. The high glucose detection of 4 at% Fe: MnO_2 indicates the superior catalytic activity than pure MnO_2.

3.4.5 Sensitivity with glucose concentration

Figure7 indicates the correlation of sensitivity between pure MnO_2 and 4 at% Fe: MnO_2 by changing the glucose concentration. It is found that both of the sensitivities change exponentially which satisfy the results reported by Hartono et al. [19] and Kondo et al. [20]. The sensor requires an elevated operating temperature to enhance redox reactions to achieve the optimum conditions. Dynamic responses of the sensor to different glucose concentrations of 0.05, 0.1, 0.3, 0.5 and 1 mol/L are shown in Figure 7. The dynamic response was not linear with respect to glucose concentrations. It is believed that at a particular concentration of $C_6H_{12}O_6$, saturation may take place due to a lack of adsorbed oxygen ions to react with analytic molecules.

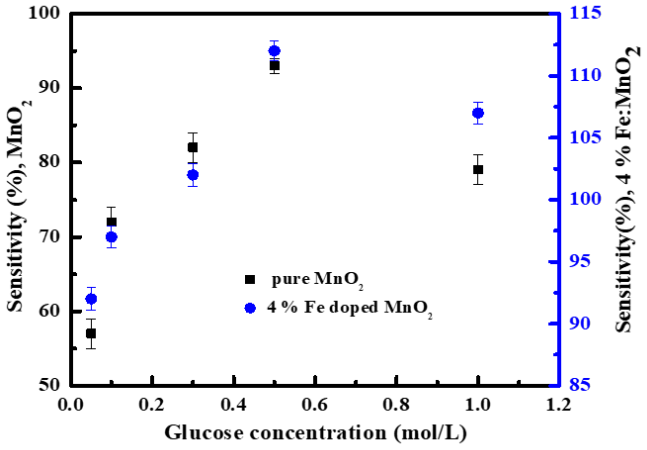

Fig.7. Glucose sensitivity of pure MnO_2 and 4at% Fe.

It is well known that in an air environment, oxygen molecules adsorb onto the surface of the nanostructured MnO_2 layer to form O_2^-, O^- and O^{2-} ions by extracting electrons from the conduction band. The oxygen adsorptions on the surface of nano oxides can be explained by the following reactions:

$$O_{2\,(gas)} \leftrightarrow O_{2(ads)}$$

$$O_{2(ads)} + e^- \leftrightarrow O^-_{2(ads)}$$

$$O_{2(ads)} + 2\,e^- \leftrightarrow 2O^-_{(ads)}$$

$$O^-_{(ads)} + e^- \leftrightarrow O^{2-}_{(ads)}$$

The positively charged MnO_2 surface and negatively charged adsorbed oxygen ions form a depletion region at the surface. Adsorbed oxygen can easily penetrate through the nanoparticle of around 20 nm diameter and so free carriers can travel through it. When the device of nanostructured MnO_2 is exposed to glucose, a complete removal of adsorbed oxygen from the nanoparticle will produce a highly conductive channel. With Fe donor, it is possible to grow n-type electron induced ferromagnetic semiconductor, to dissociate molecules and combine with the adsorbed oxygen, thus reinjecting electrons. Due to increased concentration of electrons, the depletion region decreases to produce a conductive channel along the nanoparticle, which strongly increases conductivity and thus higher sensitivity was found at 4 at% Fe: MnO_2 than pure MnO_2 thin film electrode.

4. CONCLUSIONS

The surface morphology, structural, optical and electrical properties of pure MnO_2 and Fe-doped MnO_2 thin films synthesized by a spray pyrolysis technique with different Fe concentrations of 0, 2, 4, 6 and 8 at% are investigated. The surface homogeneity of the deposited thin films increases with

Fe content due to the effect of friction among the charge carriers. The surface is consisting of agglomerated nanoparticles. The crystallite size was calculated as 20 nm at 4 at%, may be suitable for sensor developments. Moreover, small crystallite size, regularity of surface morphology, low resistivity, and high carrier concentration obtained at 4 at% Fe-doped MnO_2 thin films could be a favorable nanostructured biomedical sensor for glucose ($C_6H_{12}O_6$) response. This indicates that MnO_2 act as electrode which has better catalytic properties for the oxidation of glucose.

ACKNOWLEDGEMENTS

Muslima Zahan gratefully acknowledges the financial support approved by BUET authority for this project to conduct Ph. D research. Funding by the Ministry of Science and Technology, Government of the People's Republic of Bangladesh is also acknowledged for a Project (Project Number: 39.00.0000.09.14.009.2019/PHY'S-21/491). This publication is dedicated to the birth centenary of Bangabandhu Sheikh Mujibur Rahman, the 'Father of the nation of Bangladesh'.

REFERENCES

[1] Y. Ma, C. Fang, B. Ding, G. Ji, J. Y. Lee, Fe doped Mn_xO_y with hierarchical porosity as a high performance lithium-ion battery anode, Adv. Mater. **25**, 4646–4652, 2013.

[2] N. R. Chodankar, D. P. Dubal, A. C. Lokhande, A. M. Patil, J. H. Kim and C. D. Lokhande, An innovative concept of use of redox-active electrolyte in asymmetric capacitor based on MWCNTs/MnO_2 and Fe_2O_3 thin Films, Sci. Rep., **6**, 39205, 2016.

[3] Y. Dai, A. Molazemhosseini, K. Abbasi, C. C. Liu, A cuprous oxide thin film non-enzymatic glucose sensor using differential pulse voltammetry and other voltammetry methods and a comparison to different thin film electrodes on the detection of glucose in an alkaline solution, Biosensors, **8**(4), 1–13, 2018.

[4] K. Tian, M. Prestgard, A. Tiwari, A review of recent advances in nonenzymatic glucose sensors, Mat. Sci. Eng. C, **41**, 100–118, 2014.

[5] P. P. Sahay, A. K. Kushwaha, Electrochemical super capacitive performance of potentiostatically cathodic electrodeposited nanostructured MnO_2 films, J. Solid State Electrochem., **21**, 2393–2405, 2017.

[6] X. He, D. Hubble, R. Calzada, A. Ashtamkar, D. Bhatia, S. Cartagena, P. Mukherjee, H. Liang, A silver-nanoparticle-catalyzed graphite composite for electrochemical energy storage, J. Power Sources, **275**, 688–693, 2015.

[7] F. Mattelaer, P. M. Vereecken, J. Dendooven, and C.e Detavernier, Deposition of MnO Anode and MnO_2 cathode thin films by plasma enhanced atomic layer deposition using the $Mn(thd)_3$ precursor, Chem. Mater., **27**, 3628–3635, 2015.

[8] W. H. Bloss, F. P. Sterer, H.W. Schock, Advances in solar energy, An Annual Rev. Res. Develop., **4**, 275, 1988.

[9] K. Tian, M. Prestgard and A. Tiwari, A Review of recent advances in nonenzymatic glucose sensors, Mater. Sci. Engin. C, **41**, 100–118, 2014.

[10] G. Kim, I. Ryu, S. Yim, Retarded saturation of the areal capacitance using 3D-aligned MnO_2 thin film nanostructures as a supercapacitor electrode, Sci. Rep., **7**, 8260, 2017

[11] Y. Wang and N. Herron, Three-Dimensionally Confined Diluted Magnetic Semiconductor Clusters: $Zn_{1-x}Mn_xS$, Solid State Commun., **77**(1), 33–38, 1991.

[12] M. Zahan, J. Podder, Role of Fe doping on structural and electrical properties of MnO_2 nanostructured thin films for glucose sensing performance, Mater. Sci. Semicond. Process., **117**, 105109, 2020.

[13] W. Estrada, M. C. A. Fantini, S. C. De Castro, C. N. Polo da Fonseca, A. Gorenstein, Radio frequency sputtered cobalt oxide coating: Structural, optical, and electrochemical characterization. J. Appl. Phys., **74**(9), 5835, 1993.

[14] Z. Lihua, L. Jianbo, Y. Jianyu, G. Shenghui, P. Jinhui, Z. Libo, et al., Facile synthesis of nanocrystal tin oxide hollow microspheres by microwave-assisted spray pyrolysis method, J. Mater. Sci. Technol, **33**, 874–878, 2017.

[15] B. D. Cullity, S. R. Stock, *Elements of X-ray diffraction*, 3rd ed. Prentice Hall, New Jersey, 664 (2001).

[16] L. Xu and X. Li, Influence of Fe-doping on the structural and optical properties of ZnO thin films prepared by sol-gel method, J. Crystal Growth, **312**(6), 851–855, 2010.

[17] M. Zhang, et al., Highly sensitive glucose sensors based on enzyme-modified whole-graphene solution-gated transistors, Sci. Rep., **5**, 8311, 2015.

[18] A. J. Haider, A. J. Mohammed, S. S. Shaker, K. Z. Yahya, M. J. Haider, Sensing characteristics of nanostructured SnO_2 thin films as glucose sensor, Energy Proc. **119**, 473–481, 2017.

[19] A. Hartono, E. Sanjaya, R. Ramli, Glucose sensing using capacitive biosensor based on polyvinylidene fluoride thin film, Biosensors, **8**, 12. 2018.

[20] T. Kondo, et al., Ampherometric sensing of H_2O_2 and glucose using wet-chemically deposited MnO_2 thin films, J. Ceram. Soc. Japan, **126**, 260–262. 2018.